

A new approach to solve the Boltzmann-Langevin equation for fermionic systems

J. Rizzo,^{a,b} Ph. Chomaz,^c M. Colonna^a

^a*LNS-INFN, I-95123, Catania, Italy*

^b*Dipartimento di Fisica Universita' di Firenze, Florence, Italy*

^c*GANIL(DSM-CEA/IN2P3-CNRS), F-14076 Caen, France*

Abstract

We present a new method to introduce phase-space fluctuations in transport theories, corresponding to a full implementation of the Boltzmann-Langevin equation for fermionic systems. It is based on the procedure originally developed by Bauer et al. for transport codes employing the test particle method. In the new procedure, the Pauli principle is carefully checked, leading to a good reproduction of the correct fluctuations in the “continuum limit” ($\hbar \rightarrow 0$). Accurate tests are carried out in one and two dimensional idealized systems, and finally results for a full 3D application are shown. We stress the reliability of this method, which can be easily plugged into existing transport codes using test particles, and its general applicability to systems characterized by instabilities, like for instance multifragmentation processes.

Key words: Fluctuations; stochastic collision integral; fermionic systems; transport theories.

PACS numbers: 24.10.Cn; 24.60.Ky, 25.70.Pq

1 Introduction

In recent years, the dynamics of heavy ion collisions at intermediate energy has been extensively investigated within the framework of transport theories, such as the Nordheim approach, in which the Vlasov equation for the one-body phase space density, $f(\mathbf{r}, \mathbf{p}, t)$, is supplemented with a Pauli-blocked Boltzmann collision term [1,2]. The basic ingredients that enter the resulting transport equation, often called Boltzmann-Uehling-Uhlenbeck (BUU) equation, are the self-consistent mean-field potential and the two-body scattering cross sections. These transport models hence describe the time evolution of the

reduced one-body density in phase-space and, consequently, they are suited for the description of one-body observables, such as inclusive particle spectra in nuclear collisions, average collective flows and excitations. However, they cannot provide a reliable description of fluctuation phenomena, such as multifragmentation processes, i.e. the break-up of excited nuclear systems into many pieces. In fact, neither fluctuations of one-body observables nor many-body correlations can be addressed with this class of mean-field models. Hence suitable extensions, including fluctuations of the one-body density, have to be considered.

An intense theoretical work on fluctuations in nuclear dynamics has started in the past years, also stimulated by the availability of large amounts of experimental data on fragment formation in intermediate energy heavy ion collisions and the possibility to observe a liquid-gas phase transition [3,4,5,6,7,8,9]. In order to introduce fluctuations in transport theories, a number of different avenues have been taken, that can be essentially reconducted to two different classes of models. One is the class of molecular dynamics models [9,10,11,12,13,14] while the other kind is represented by stochastic mean-field approaches [16,17,8].

In molecular dynamics models the many-body state is represented by a simple product wave function, with or without antisymmetrization. The single particle wave functions are assumed to have a fixed Gaussian shape. In this way, though nucleon wave functions are supposed to be independent (mean-field approximation), the use of localized wave packets induces many-body correlations both in mean-field propagation and hard two body scattering (collision integral), which is treated stochastically. Hence this way to introduce many-body correlations and produce a trajectory branching is essentially based on the use of empirical gaussian wave packets. If wave functions were allowed to assume any shape, the method would become identical to standard mean-field descriptions. While the wave function localization appears appropriate to describe final fragmentation channels, where each single particle wave function should be localized within a fragment, the use of fixed shape localized wave packets in the full dynamics could affect the correct description of one-body effects, such as spinodal instabilities and zero sound propagation [14,15].

On the other side, in the so-called stochastic mean-field approaches, the stochastic extension of the transport treatment for the one-particle density is obtained by introducing a stochastic term representing the fluctuating part of the collision integral [16,17], in close analogy with the Langevin equation for a brownian motion. This can be derived as the next-order correction, in the equation describing the time evolution of f , with respect to the standard average collision integral, leading to the Boltzmann-Langevin (BL) equation. Thus, the system is still described solely in terms of the reduced one-body density f , but this function experiences a stochastic time evolution in response to the

random effect of the fluctuating collision term. In this way density fluctuations are introduced, that are amplified when instabilities or bifurcations occur in the dynamics. This procedure is suitable also for addressing multifragmentation phenomena, since fragments can be associated with the regions where the spacial density becomes larger, which finally can be reconstructed by sampling the one-body distribution function.

A specific method for solving the Boltzmann-Langevin equation by direct numerical simulation was introduced in Refs.[18,19]. In this numerical implementation, the one-particle density $f(\mathbf{r}, \mathbf{p})$ is represented on a lattice of grid points in phase space and the collision integral is treated by considering all possible transitions between phase space cells, adding a noise term whose features are related to the average rate of transitions between two specified initial cells and two final cells. The numerical implementation of this method has only been possible in two dimensions (2D) because it requires too large computer resources in 3D.

Hence several approximate solutions of the BL equations have been formulated, mostly based on the projection of the BL noise only on a given dynamical variable (such as the local quadrupole tensor of the momentum distribution) or on \mathbf{r} space only [20,21]. More tractable fluctuating terms, such as a stochastic force added to the mean-field potential, have also been proposed and extensively applied to multifragmentation studies [22,7,8].

However, the implementation of the full structure in phase space of the original BL term can still be considered as an important goal to reach. In fact, this would allow to treat a more general class of phenomena, where the correct description of fluctuations and correlations in \mathbf{p} space is essential (such as particle production and fragment velocity correlations for instance). Moreover, also in the multi-fragmentation mechanism, that is dominated by spacial density fluctuations, a more accurate representation of the full phase space dynamics, including fluctuations, would allow to improve the description of the fragment kinematical properties and correlations.

We also stress the general interest of this effort. Indeed transport phenomena occur in many physical systems, for which a more precise description of the time evolution of the one-body distribution function, including the effect of many-body correlations, would be important.

A first attempt to introduce a fluctuating collision term in a 3D transport approach was made by Bauer et al. [23]. This method can be implemented relatively easily into standard transport codes that adopt the scattering of pseudo-particles (or test particles) as a method of solution of the collision integral and it consists essentially in forcing similar two-body collisions to occur for neighboring test particles, defined according to a given distance in phase

space, so that effectively two nucleons are involved in each particular collision event. The distance should reproduce the phase-space shape of the nucleon wave function. In this way the random nature of the two-body scattering, that in the standard codes applies only to test particles and is washed-out when using a huge number of them, is transferred to entire nucleons. However, in the procedure proposed in Ref.[23] the Pauli blocking is checked only for the collision of the two original test particles and not for the entire swarm affected, leading to some unpleasant features in the description of fermionic systems. Indeed the Pauli-blocking violation introduces important inaccuracies in the fluctuations of the one-body density.

In the present manuscript we present a new method to reconstruct the phase space nucleon wave function in mean-field approaches, in such a way that the Pauli-blocking is checked for the entire cloud of moved particles. This will improve the description of the fluctuation variance, approaching the one expected for fermionic systems. We will also pay special attention to the definition of the phase-space metric that would optimize the value of this variance.

The paper is organized as follows: We will first recall the main ingredients of the BL theory, in order to connect the formalism with the numerical implementation adopted (Section 2). Then we will discuss in more detail the methods that have been proposed so far to solve the Boltzmann-Langevin equation (Section 3). The new procedure that we follow to build fluctuations is presented in Section 4. Several results demonstrating and analyzing in detail the method are discussed from Section 5 to 8. Conclusions and perspectives are drawn in Section 9.

2 The Boltzmann-Langevin equation

Within the semi-classical framework, the stochastic transport equation of motion for the one-body distribution function f can be expressed in the following form,

$$\dot{f} \equiv \frac{\partial}{\partial t} f - \{h[f], f\} = K[f] = \bar{K}[f] + \delta K[f], \quad (1)$$

where the left side describes the collisionless propagation of the individual particles in their common self-consistent one-body field, while the right side expresses the effect of the residual binary collisions.

The collision term $K[f]$ has a stochastic character. For example, the distance a particle travels in the medium before colliding is stochastic, as is the resulting scattering angle. At the Boltzmann level, Eq.(1) includes only the *average* part of the collision term, $\bar{K}[f]$. Usually, in nuclear systems, the quantum statistics is taken into account by adding suitable Fermi blocking in the

single-particle final states, leading to the Uehling-Uhlenbeck collision term [24,25]. The resulting nuclear Boltzmann equation exists in many implementations that differ with respect to both the physical input (such as the types of constituents included, the form of their effective Hamiltonian, and their differential interaction cross sections) and the numerical methods employed (whether of test particle or lattice type) and various names have been employed in the literature, including BUU (for Boltzmann-Uehling-Uhlenbeck), VUU (for Vlasov-Uehling-Uhlenbeck), Landau-Vlasov and BNV (for Boltzmann-Nordheim-Vlasov) [1,2,26,27,28]. The Boltzmann-Langevin treatment includes also the *stochastic* part of the collision term, $\delta K[f]$ [16,17].

In the simple physical scenario where the residual interaction can be considered as binary collisions that are well localized in space and time, the average part is given by [24,25]:

$$\bar{K}(\mathbf{r}, \mathbf{p}_1) = g \sum_{234} W(12; 34) [\bar{f}_1 \bar{f}_2 f_3 f_4 - f_1 f_2 \bar{f}_3 \bar{f}_4] , \quad (2)$$

where f_i is a short-hand notation for $f(\mathbf{r}, \mathbf{p}_i, t)$ and $\bar{f} \equiv 1 - f$ is the associated Fermi blocking factor. g is the degeneracy factor.

The basic transition rate is simply related to the differential cross section for the corresponding two-body scattering process,

$$W(12; 34) = v_{12} \left(\frac{d\sigma}{d\Omega} \right)_{12 \rightarrow 34} \delta(\mathbf{p}_1 + \mathbf{p}_2 - \mathbf{p}_3 - \mathbf{p}_4) , \quad (3)$$

being $v_{12} \equiv |\mathbf{v}_1 - \mathbf{v}_2|$ the relative velocity, and it thus has corresponding symmetry properties,

$$W(12; 34) = W(21; 34) = W(34; 12) . \quad (4)$$

Since it arises from the same elementary two-body processes, the stochastic part of the collision term is fully determined by the basic transition rate as well, as a manifestation of the fluctuation-dissipation theorem. With the collisions assumed to be local in space and time, the correlation function for the fluctuating part of the collision term has the following form,

$$\prec \delta K(\mathbf{r}, \mathbf{p}_1, t) \delta K(\mathbf{r}', \mathbf{p}_1', t') \succ = C(\mathbf{p}_1, \mathbf{p}_1', \mathbf{r}, t) \delta(\mathbf{r} - \mathbf{r}') \delta(t - t') , \quad (5)$$

where $\prec \cdot \succ$ denotes the average with respect to the ensemble of possible trajectories resulting from the current one-body density f . Furthermore, for elastic scattering, the correlation kernel is given by [16]:

$$C(\mathbf{p}_1, \mathbf{p}_1', \mathbf{r}, t) = \delta_{11'} \sum_{234} W(12; 34) F(12; 34)$$

$$+ \sum_{34} [W(11'; 34)F(11'; 34) - 2W(13; 1'4)F(13; 1'4)] , \quad (6)$$

with the short-hand notations $\delta_{11'} \equiv h^D \delta(\mathbf{p}_1 - \mathbf{p}'_1)$ and $F(12; 34) \equiv f_1 f_2 \bar{f}_3 \bar{f}_4 + \bar{f}_1 \bar{f}_2 f_3 f_4$ (D is the dimension of the space considered). The symmetry properties (4) of the transition rate ensure that the following sum rules hold,

$$\sum_1 C(\mathbf{p}_1, \mathbf{p}_2, \mathbf{r}, t) = \sum_2 C(\mathbf{p}_1, \mathbf{p}_2, \mathbf{r}, t) = 0 , \quad (7)$$

$$\sum_1 C(\mathbf{p}_1, \mathbf{p}_2, \mathbf{r}, t) \mathbf{p}_1 = \sum_2 C(\mathbf{p}_1, \mathbf{p}_2, \mathbf{r}, t) \mathbf{p}_2 = \mathbf{0} , \quad (8)$$

$$\sum_1 C(\mathbf{p}_1, \mathbf{p}_2, \mathbf{r}, t) \epsilon_1 = \sum_2 C(\mathbf{p}_1, \mathbf{p}_2, \mathbf{r}, t) \epsilon_2 = 0 , \quad (9)$$

where $\epsilon_i = p_i^2/2m$ is the kinetic energy for a specified momentum. These sum rules express the fact that each of the elementary binary collisions conserves particle number, momentum, and energy, respectively.

3 Methods to solve the BL equation

3.1 Lattice calculations

The numerical implementation of the Boltzmann-Langevin equation is accomplished by correctly simulating the basic stochastic process, i.e. the stochastic transition rate among phase-space cells. One can realize that this point is very delicate in finite systems, when we work with a relatively small number of nucleons, but still need to build a smooth distribution function. There are different ways to overcome this difficulty.

As mentioned in the Introduction, one possibility, proposed in Ref.[18], is to solve the BL equation on a lattice; phase space is therefore divided into a number of cells, each one having volume $\Delta s = \Delta \mathbf{r} \Delta \mathbf{p}$ (s denotes a point in phase space: $s \equiv (\mathbf{r}, \mathbf{p})$).

Each transition involves four locations, and the collision integral arises from the sum of the transitions evaluated for all possible combinations of the cells: from this consideration one recognizes that the practicality of the method is limited by the huge computational effort required. In fact, only two-dimensional implementations exist [18,19]. Each transition represents a basic stochastic process, and, following the BL theory, the actual number of such transitions in a time step Δt is dispersed around the mean value according to a Poisson

distribution, so its variance amounts to:

$$\sigma_{\nu}^2 = \bar{\nu}, \quad (10)$$

where the average is given by:

$$\begin{aligned} \bar{\nu}(12; 34) &= \frac{\Delta s_1}{h^D} \frac{\Delta s_2}{h^D} \frac{\Delta s_3}{h^D} \frac{\Delta s_4}{h^D} f_1 f_2 \bar{f}_3 \bar{f}_4 W(12; 34) \\ &\cdot \delta(\mathbf{r}_1 - \mathbf{r}_2) \delta(\mathbf{r}_1 - \mathbf{r}_3) \delta(\mathbf{r}_2 - \mathbf{r}_4) \Delta t. \end{aligned} \quad (11)$$

This is a compact form of the fluctuation-dissipation theorem, since it predicts that the fluctuations are simply related to the mean number of dissipative processes. Then, a noise term $\delta\nu(12; 34)$ is added to the mean number $\bar{\nu}(12; 34)$, and thus the actual number of transitions is a random number picked from a normal distribution, the center of which is the mean value, and where the width is given by Eq.(10). In refs. [19,29] this procedure is proven to yield correct results for a 2D system of fermions interacting through hard two-body scattering. Starting from a non-equilibrium situation (two touching Fermi spheres) the method is successful in reproducing the expected fluctuations, preserving also the average trajectory of the system. In particular, the fluctuations introduced build the expected statistical value for the equilibrium one-body density variance:

$$\sigma_f^2(s) = \prec \delta f(s) \delta f(s) \succ = f_{eq}(s) \bar{f}_{eq}(s) h^D / (g \Delta s), \quad (12)$$

evaluated considering phase-space cells of volume $\Delta s = h^D$, for which the fluctuating transition rate is implemented. Here $f_{eq}(s)$ denotes the equilibrium value of the one-body distribution function and $\delta f(s) = f(s) - \prec f(s) \succ$. Of course, Eq.(12) holds also for volumes larger than h^D and fluctuations are scaled accordingly. Also the co-variance, i.e. the correlation between density fluctuations in two different phase-space points, s and s' , is well reproduced [19].

The same authors of Ref.[19] also verified that, for the same idealized system, but prepared at low spatial density, early fluctuations developed in momentum space are subsequently transmitted into density fluctuations and amplified by the nuclear mean field [30], leading to large instabilities and a statistical population of fragments.

3.2 The pseudo-particle correlation method

The method of Ref.[18] was originally developed as a way to overcome the problems arising from the solution of transport equations with the test particle method, which we now discuss briefly. Within the test particle method, each

nucleon is represented by a collection of N_{test} test particles, that are propagated according to the mean-field interaction and random two-body scattering. The use of a large number of test particles allows to have a smooth distribution function and a good coverage of the phase space for the Pauli blocking. On the other side, since collisions are treated stochastically for the single test particles, the dispersion around the average number of nucleon collisions (Eq.(10)) is automatically divided by N_{test} . Hence fluctuations which are introduced by the test particle algorithm can also be seen as the correct ones expected from the BL approach, divided by the factor N_{test} .

Various paths have been followed to overcome this problem. For instance, one can choose $N_{test} = 1$, i.e. work with whole nucleons [10], but in this case one has to solve the problem of the induced numerical errors on the smooth path of the dynamics, i.e. the mean-field and the Pauli-blocking factors. Alternatively, Bauer et al. proposed a method to introduce a correlation between close particles in phase-space [23].

The method follows the idea, applied in extended Time-Dependent-Hartree-Fock (TDHF) calculations, of evolving the single-particle density including a statistical mixing of Slater determinants [31]. The jump from one configuration to the other is possible under the important assumption that any coherence between determinants can be ignored (decorrelation approximation). The choice of the single-particle basis for the determinant is however somewhat arbitrary, apart from the requirement of momentum-energy conservation. These ideas can be translated into the semi-classical approximation using the test particle method. The mixing between Slater determinants is realized in the collision integral by means of the following procedure.

- (1) First of all, the nucleon-nucleon (NN) cross section is reduced by a factor N_{test} .
- (2) Then two test particles i_1 and i_2 are chosen as colliding partners, and will be moved from their positions \mathbf{p}_1 and \mathbf{p}_2 , to new positions \mathbf{p}_3 and \mathbf{p}_4 , according to the corresponding transition probability including the Pauli blocking of the final states [2].
- (3) If the two particles can collide, the scattering actually involves two “clouds” of neighbouring test particles, corresponding to two entire nucleons ($2 \times N_{test}$ particles). The contiguity criterion is based on the following definition of phase-space distance:

$$d_{ij}^2 = (\mathbf{p}_i - \mathbf{p}_j)^2/p_F^2 + (\mathbf{r}_i - \mathbf{r}_j)^2/R^2 \quad (13)$$

where p_F is the Fermi momentum and R is the radius of the considered system. (It should be noticed that the choice of this phase-space metric is rather arbitrary).

- (4) In order to ensure energy and momentum conservation, the final states are adjusted using the average momenta of the two clouds as initial states.

Two important remarks have to be done:

- the Pauli blocking is checked only for the collision of the test particles i_1 and i_2 and not for each particle of the cloud. We will see in the following that this choice induces a strong violation of the Pauli principle;
- the effect of the collision is a mere translation (in momentum space) of the two clouds to final positions, as sketched in Fig. 1.

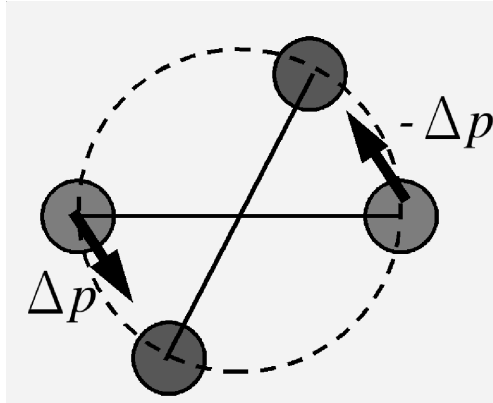


Fig. 1. Illustrative picture of nucleon-nucleon scattering in the pseudo-particle correlation method.

This method is conceptually simple, and moreover the implementation into existing BUU or BNV codes is really straightforward. Indeed it was immediately used to test the effects of the fluctuations on fragment mass spectra in a $^{20}\text{Ne} + ^{20}\text{Ne}$ reaction at 100 AMeV [23].

Its validity has been checked later by Chapelle et al. [29], for the same idealized 2D system for which the BL lattice simulation method was implemented. Accordingly, a different metric, involving only distances in momentum space, was used. As shown in [29], the final equilibrium value obtained for the fluctuation variance does not reproduce the expected one. The variance profile, as a function of the energy, appears to be proportional to f_{eq} rather than to $f_{eq}\bar{f}_{eq}$. Actually, this would be the result for a classical system, obeying to the Boltzmann statistics. This can be considered as a consequence of the fact that Pauli blocking is checked only for the first two colliding partners, and the system progressively evolves towards an equilibrium configuration which is more consistent with the one of a classical system.

From this discussion it is evident that a proper treatment of the Pauli blocking is a fundamental requirement for any numerical implementation of the Boltzmann-Langevin theory for fermionic systems. However, apart from these problems, the pseudo-particle correlation method represents a simple and practical way to implement fluctuations into transport codes. Therefore, it is worthwhile to think about some improvements to make it more accurate. This is the aim of the present work, as we will discuss in the next Section.

4 The improved pseudo-particle correlation method

The method devised by Bauer et al. is able to agitate the phase space function and build fluctuations, although their strength does not reproduce the expected value for fermionic systems. However, a careful modification of the original procedure can considerably improve the results.

The new procedure can be summarized in the following steps:

- (1) The choice of the two colliding partners closely traces the standard recipe. If the two test particles are allowed to collide, two clouds of N_{test} particles will be moved, with conditions specified below.
- (2) Only particles within a sphere, in coordinate space, around the center of mass of the two partners i_1 and i_2 can belong to the clouds. The distance criterion is $|\mathbf{r}_i - \mathbf{r}_{CM}(i_1, i_2)| < d_r$, where d_r is a free parameter (see later discussion). Then, for this considered space sphere, a grid is introduced in momentum space, around i_1 and i_2 , the size of each cell being V_{cell} .
- (3) Given the momentum space cells I and J containing the partners i_1 and i_2 , we consider the cells I' and J' , corresponding to the final positions, in a rotated frame, as indicated in Fig. 2. For a given set of initial and final cells, the number of test particles that will be actually moved to final states is equal to the minimum between the occupation of the initial cells, n , and the availability of the final ones $\bar{n}' = (N_{max} - n')$:

$$n_t(I, I'; J, J') = \min(n_I, n_J, \bar{n}_{I'}, \bar{n}_{J'}),$$

where $N_{max} = gV_r V_{cell}/h^D$ is the maximum number of test particles that can stay inside a cell. It should be noticed that this choice corresponds to the maximum of possible moves.

- (4) Surrounding momentum space cells are searched with the same prescriptions, until two entire nucleons are found. The search procedure is symmetric with respect to the center of momentum of the two partners and random in the vicinity of the original cells (I,J).
- (5) Finally, the two clouds are moved to the new states of the rotated frame (see Fig.2), so that the conservation of energy and momentum is automatically obtained. However, a further check is performed. In fact, due to the finite number of test particles, the one-body density is not perfectly homogeneous inside each cell. This causes slight violations of the conservations laws. Hence the origin of the momentum space grid is eventually slightly displaced in order to have a perfect energy and momentum conservation.

This method involves two parameters, namely the radius of the sphere in \mathbf{r} space, d_r , and the size of the momentum cells, V_{cell} . The radius d_r fixes the spatial extension of the nucleon, that in turn influences its spreading in

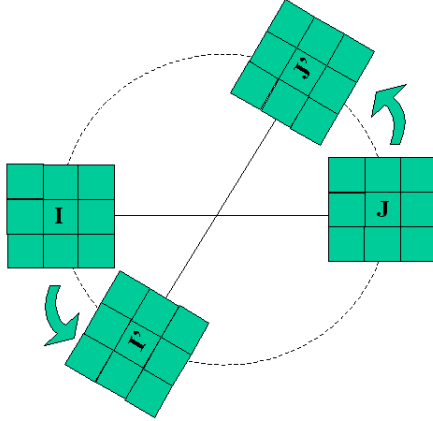


Fig. 2. Schematic picture of the collisional procedure in the improved pseudo-particle correlation method.

momentum space. Hence this parameter fixes somehow the extension of the nucleon wave packet in phase-space and could affect the transport dynamics. It can be constrained by physical arguments, and in general it should depend on the physical properties of the system, such as its dilution.

4.1 General comments

The method proposed here has several advantages with respect to the original one of Ref. [23]. It is still very flexible, and can be easily implemented into existing transport codes; moreover, it is quite fast, and does not require huge amounts of resources. The Pauli blocking is locally checked in each collision, so in principle this procedure satisfies the basic requirements to preserve the average evolution and to yield the expected fluctuations. Besides, differently from the original method, where the nucleon is essentially spherical in phase space, here it is allowed to assume any shape in momentum space, since the only restriction is given by the cell size V_{cell} . In other words, it is possible to take into account momentum deformations of the nucleon wave packet, due to the momentum distribution of the system in particular conditions. For instance, when equilibrium is approached, the Pauli principle allows collisions essentially for nucleons lying on the surface of the Fermi sphere; therefore such nucleons should not have a spherical shape in momentum space.

It is also interesting to make a connection between the proposed method and the lattice simulation method to build fluctuations.

The numerical procedure described in Ref. [18], where the phase space is discretized by a fixed grid of cells, allows to construct the correct value of the fluctuation amplitude in each cell of the grid, generally taken of volume h^D (but in principle it can be even smaller), on the basis of the fluctuating gain

and loss terms.

On the other hand, our procedure is based on a different philosophy: Instead of constructing fluctuations in fixed cells, when a collision occurs we move all together the phase space volume containing one nucleon. The shape of this volume is not fixed a priori and depends on the location of the four points $(\mathbf{p}_1, \mathbf{p}_2, \mathbf{p}_3, \mathbf{p}_4)$ that have been chosen as initial and final centroids of the considered two-body collision. This means that the “correlation volume”, i.e. the volume of the sphere that envelops all test particles that move all together in each collision, is not fixed, but has to be considered as a dynamical variable that generally exceeds h^D and could even reach rather large values. In other words, compared to what is done in Ref. [18], we build fluctuations in volumes containing one nucleon, but these volumes do not correspond to single cells of a fixed grid: instead, their contour changes from one collision to another, according to the prescription adopted to construct the clouds around the two first colliding test particles i_1 and i_2 .

But how can the two proposed methods be connected to the original BL equation ? It should be noticed that the Boltzmann-Langevin equation (1) is a semi-classical equation, derived in the “continuum limit” ($h \rightarrow 0$). This implies that the evolution of the system under consideration is completely determined by a smooth distribution function, i.e. it behaves as a fluid in phase space. In other words, the volume Δs of the phase space cells for which the fluctuating transition rate is evaluated, is supposed to be much larger than h^D . The Boltzmann-Langevin equation is essentially based on the idea of a fluctuating collision rate among phase space cells containing many nucleons. The formalism does not provide any additional information about the “structure”, i.e. the shape of the single nucleon wave packet.

In both numerical implementations described above, two-body collisions among nucleons are treated as a stochastic process. Only the definition of nucleon wave packet and/or of the elementary cells where fluctuations are built change from one method to the other. As discussed above, this ingredient is not contained in the BL equation and such information is beyond its derivation. Hence, both procedures can be considered as correct implementations of the Boltzmann-Langevin theory in the “continuum limit”, the definition of “nucleon wave packet” being rather arbitrary.

However, it is also very interesting to investigate the differences between the various possible methods used to build the nucleon clouds, that in turn influence the correlation volume. In particular, one can also try to force the procedure in order to reduce the wave packet smearing and to correlate particles inside smaller volumes (close to h^D).

4.2 Details of the model

In the present first implementation of the method, similarly to what was done for the lattice simulations of Ref.[19], we neglect the evolution in coordinate space, extending d_r to the whole coordinate space. The cell size V_{cell} is then constrained by the following arguments: it should be small enough to allow an accurate check of the Pauli blocking, but large enough to contain a sufficient number of test particles to reduce numerical uncertainties. In any case, V_{cell} has not to exceed the volume where, at most, one nucleon can be accommodated: $V_p = h^D/(gV_r)$, being V_r the volume in the coordinate space ($V_r = \frac{4}{3}\pi d_r^3$). In the following we take $g = 1$, unless expressly indicated. Since we neglect the coordinate space, we will refer only to volumes V in momentum space. The expected equilibrium value of the variance σ_f^2 in such volumes is:

$$\sigma_f^2 = f_{eq} \bar{f}_{eq} \frac{V_p}{V} = \frac{f_{eq} \bar{f}_{eq}}{N_V} \quad (14)$$

where N_V is the number of nucleons that can be accommodated, at most, in the considered volume V . It should be noticed that, according to our procedure to build the nucleon wave packet, the expected value of fluctuations, (Eq.14), can be reproduced only in volumes V larger than the average correlation volume, while it is underestimated in smaller cells, since fluctuations are built on a larger scale.

4.3 Illustrative results

In order to illustrate how our procedure works, we will first consider the very simple case of particles moving only along one direction. We take a large system, containing 1000 nucleons with average occupancy $\langle f \rangle = 0.5$. So the total extension in momentum space of the system is $2000 \times V_p$. Then the system is divided into $N = 4000$ smaller cells that can contain at most half nucleon, whose occupancy can be either 0 or 1. Hence $V_{cell} = V_p/2$. The occupancy is randomly chosen at the beginning and collisions are performed until equilibrium has been reached. The initial (p_1, p_2) and final (p_3, p_4) states of a collision are chosen randomly among the N cells. We neglect energy and momentum conservation in this simple example. Moreover, for simplicity, we take $p_2 = -p_1$ and $p_4 = -p_3$. Hence only half of the considered space is independent and, in this situation, the probability for a collision to happen is proportional to the product $f(p_1)(1 - f(p_3))$. According to Eq. (14), the expected fluctuation value, in a given momentum space volume V , will be $\sigma_0^2 = 0.25 V_p/V$. The general prescription (see Sect. 4) states that when a collision happens, a full nucleon has to collide. Therefore, we move together the cell i and the closest occupied cell that finds an empty cell in the final

position. This example can be seen as a simple implementation of the general procedure when considering nucleons represented by only two test particles. One can easily realize that the “correlation radius”, i.e. the distance between the two cells that move together, changes from one event (collision) to another: sometimes the two co-moving cells are neighbours, sometimes they can be rather far. Of course, for practical reasons, we have to restrict our search within a given radius. For instance, considering 10 cells on each side (with respect to i), we are able to reconstruct the nucleon and to perform the collision in more than 98% of the cases.

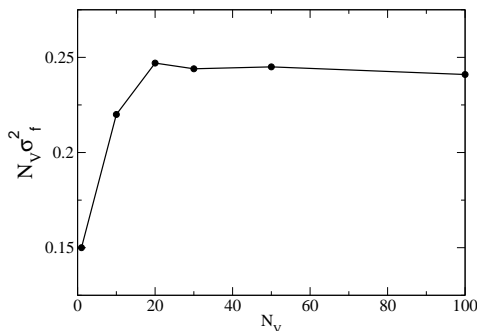


Fig. 3. Variance of the distribution function as a function of the number N_V (see text), in the idealized case of particles moving only along one direction.

In Fig. 3 we present the results for the fluctuation variance as a function of the number N_V of “nucleon” cells (of volume V_p) that are contained inside the volume V where the function f is evaluated. One thousand events have been considered. The fluctuation value presented in the Figure is multiplied by N_V . As one can see in the Figure, the correct value of the fluctuations, i.e. $N_V \sigma_0^2 = 0.25$, is approximately recovered (within $\sim 5\%$) for volumes $V \approx 20 V_p$. The slight deviation is due to the upper bound considered for the “correlation radius” and to the constraints imposed by the total mass conservation, that are also responsible for the decrease of fluctuations observed for large N_V values.

From this simple example, it already appears that the exact fluctuation value ($N_V \sigma_0^2 = 0.25$) is reached only asymptotically. This is due to the arbitrariness of the nucleon shape and of the centroid position. Hence, when testing a given procedure to solve the stochastic collision integral, the resulting fluctuations have to be compared to the expected values in large volumes, in which all different possibilities (nucleon configurations) may be accommodated.

These considerations would apply also to the original procedure proposed by Bauer et al. Thus, in Ref.[29], the comparison between the obtained fluctuation variances and the expected ones should have been done considering also volumes containing many nucleons, and not only cells of volume V_p where, as seen in Fig.3, fluctuations are naturally suppressed by the fact that the

nucleon wave packet may take any shape. However, this does not affect the conclusions drawn in [29], mainly based on the wrong profile of the density variance (and not on its absolute value).

In the next Section we will move to describe more complex geometries and different procedures to build the nucleon wave packets.

5 Fluctuations of a Fermi gas: Analysis on the Fermi surface

Here we will discuss our procedure to build fluctuations in the context of a system of fermions having a given density and temperature, i.e. initialized according to a Fermi-Dirac distribution. This is a situation that is easily reached in the course of a dissipative nuclear reaction, after the initial collisional shock [8]. Since collisions happen mostly on the Fermi surface, let us first consider only particles within a thin stripe dp around the Fermi momentum, where $\langle f \rangle = 0.5$.

For those colliding particles the relative velocity v_{12} is constant, since only particles with opposite momenta can collide, in order to stay on the Fermi surface. So the transition rate is essentially governed by the product $f_1 f_2 \bar{f}_3 \bar{f}_4$.

This simplified system will allow us to study the sensitivity of the results to the ingredients of the procedure used to build, step by step, the nucleon clouds. As also discussed before, we will show that the correct fluctuation amplitude is recovered in the “continuum limit”, i.e. in large volumes. However, in the following we will mostly concentrate on the fluctuation amplitude in volumes of size V_p , in order to probe the extension of the nucleon wave packet. The latter could influence significantly the evolution of actual nuclear collisions, where it could be important to work with more compact nucleon configurations.

Using this simple model we will find that building the maximum fluctuation value (e.g. $\sigma_0^2 = 0.25$) in such a volume, i.e. correlating particles inside V_p , is a quite difficult task and additional efforts are required in order to reduce the nucleon cloud smearing.

5.1 Details of the simplified model

In order to keep the particles on the Fermi surface, the original procedure described in Sect. 4 was slightly modified so that the modulus of the momentum of the particles does not change: only particles belonging to cells with opposite momenta can collide. Then, for symmetry reasons it will result $f(\mathbf{p}_1) = f(\mathbf{p}_2 = -\mathbf{p}_1)$. The transition probability finally depends only on two

values of the distribution function, $f(\mathbf{p}_1)$ and $f(\mathbf{p}_3)$. We use spherical coordinates $(\cos(\theta), \phi)$ as independent variables. The collision partners of particles in the cell $(\cos(\theta), \phi)$ will be the ones in the cell $(\cos(\pi-\theta), \pi+\phi)$. The choice of these coordinates implies the grids used in the procedure to be fixed along the $\cos(\theta)$ axis. They can slide along the ϕ axis, where periodic conditions are taken into account.

The procedure is as follows: a test particle i_1 is chosen at random (together with the corresponding partner i_2) and a grid is constructed, centered around i_1 and i_2 (see Fig.2). The rotation angles, also taken from a flat distribution, fix the final states and the new frame corresponding to these final positions.

We consider a shell with 40×40 cells, whose size is chosen to accommodate one nucleon at most, so that $V_{cell} = V_p$. We have checked that the results do not depend on the number of cells, i.e. the number of nucleons considered, by performing the same calculations on a 64×64 system. We use 500 test particles per nucleon.

The growth of fluctuations is described by the variance σ_f^2 of the distribution function, as discussed before. Usually it is evaluated performing an ensemble average over a large number of events having the same initialization. However, in this scheme the mean value $\langle f \rangle$ does not depend on the position \mathbf{p} and is not changing in time. Considering the large number of cells employed, we can also follow the evolution of the system by calculating in a single event the following quantity:

$$\sigma_f^2 = \langle (f_i - \langle f \rangle)^2 \rangle_{cells}, \quad (15)$$

where $\langle \cdot \rangle$ denotes the average with respect to the cells and $\langle f \rangle = 0.5$.

5.2 “Fixed grid” calculations

In order to understand how the recognition of the nucleon wave packet can be influenced by the details of our procedure, we first further simplify the problem by using a single fixed grid to make the collisions, i.e. test particles are placed at (and can only move to) the center of the cells of the grid. In this case we have a single reference frame, so the effect of a collision (in the space $(\cos(\theta), \phi)$) is a mere translation to other states of the same grid. Apart from the use of test particles, and related differences in the method followed to solve the collision integral, in this way the procedure becomes similar to the one used in Ref. [18].

We will take, as initial conditions, f strictly equal to 0.5 in each cell of the fixed grid, corresponding to 800 nucleons. By construction, once collisions are performed, the only possible values for f are 0, 0.5 and 1.

The maximum fluctuations in V_p ($\sigma_0^2 = 0.25$) would be reached only if, in each cell, f is either zero or one. Achieving this result is not a trivial task: Cells starting with $f = 1$ can be partially emptied, and cells with $f = 0$ partially filled.

The dot-dashed curve in Fig.4, upper panel, shows the variance of the distribution function calculated in the cells of the fixed grid, with increasing number of collisions (i.e. as a function of time). It saturates approximately when almost all nucleons have suffered one collision. In the equilibrium configuration the number of cells with the three possible values of f is roughly the same, as shown in Fig. 4 (lower panel), so the fluctuation variance is $\sigma_f^2 \approx 0.175$, which is about 2/3 of the maximum.

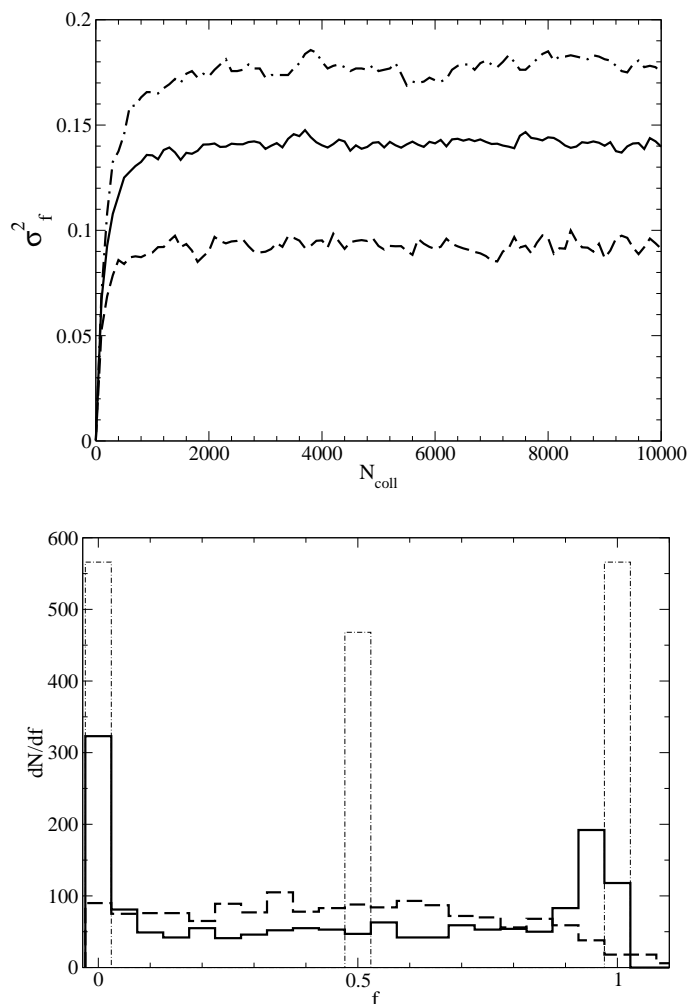


Fig. 4. Upper panel: variance of the distribution function in V_p , as a function of the number of collisions, for three different cases: fixed grid with $f(t = 0) = 0.5$ (dot-dashed), fixed grid with randomly distributed test particles (full), moving grid (dashed). Lower panel: Distribution of the number of cells as a function of their occupation f at equilibrium, for the three cases indicated above.

The fluctuations reached in V_p also depend on the variance of the initial configuration. If we initialize the system distributing the test particles randomly, the occupation in the cells has an average value $\langle f \rangle = 0.5$ and a width given by $\sigma_f(t=0)/\langle f \rangle = \bar{N}^{-1/2}$, where \bar{N} is the average number of test particles per cell ($\bar{N} = 250$). The distribution function can assume any value between 0 and 1, as shown by the full curve in Fig. 4, lower panel. The initial continuous distribution of values of f causes a reduction of the fluctuations in V_p (full curve in Fig. (4), upper panel) with respect to the previous case. As expected, the fact that f varies continuously between 0 and 1 contributes to enhance the smearing of the nucleon wave packet and hence to reduce fluctuations in V_p .

5.3 The centroid degree of freedom

Now we turn to a more general situation, relaxing the condition of the fixed grid. Hence here we would like to test the full procedure, described in Section 4, that we will finally follow in the full 3D case. The two reference frames used to make the collision (the one concerning the initial states and the one for the final states) are now shifted along the ϕ axis, since the angle ϕ of the initial and final states can assume any value between 0 and 2π , according to the initial and final positions of the colliding test particles, i_1 and i_2 .

This carries two important consequences. First of all, even being the Pauli blocking checked for each collision in a particular frame, the prescription $f \leq 1$ can be violated in another frame. However, we checked that this violation concerns only about 5% of the cells. Second, the correlation between the cells representing the reconstructed nucleon, which is maximum in the search frame, will be systematically broken in another (shifted) reference frame, increasing the nucleon delocalization and thus reducing fluctuations in V_p .

The dashed curve in Fig. 4 shows the fluctuations obtained in V_p in this case. Since this feature is due to the arbitrary position of the centroid of the constructed nucleon with respect to a fixed reference frame, we will name it *centroid effect*. We notice a fluctuation reduction of $\sim 60\%$ with respect to the fixed grid case (dash-dotted line in the same Figure).

5.4 Sensitivity to the dimension of the grid cell

Up to now, the step of the grid has been chosen so that $V_{cell} = V_p$. However, in general, the size of the search cell has to be smaller than V_p , especially when the nucleon wave packet is rather delocalized in \mathbf{p} space (being more compact in coordinate space). In fact, small search cells are required for the Pauli

blocking to be accurate. Hence we want to study the sensitivity of the results to the size of the search cell. Let us start with the fixed grid scheme. In Fig. 5 we plot the fluctuation variance obtained dividing the step in the ϕ direction, ϕ_{step} , by two or four; the volume of the search cell is then $V_{cell} = V_p/2, V_p/4$, respectively. This is equivalent to shift, for each collision, the origin of the grid by 0.5 or 0.25 ϕ_{step} respectively, and acts also as a sort of centroid effect, thus reducing the variance in V_n (see solid and dashed lines in Fig. 5). The

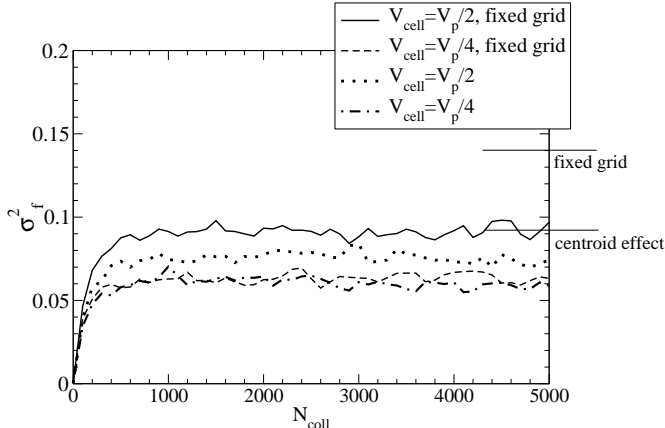


Fig. 5. Variance of the distribution function in the fixed grid scheme and in the general case, for two sizes of the search cell. The lines on the right indicate the values for $V_{cell} = V_p$, also shown in Fig. 4.

value obtained with $V_{cell} = V_p/2$ is lower than the corresponding case with $V_{cell} = V_p$, indicated as “fixed grid” in the Figure. Moreover, it further reduces for $V_{cell} = V_p/4$. Nevertheless, this smearing effect is partly compensated by the fact that the procedure used to select the cells belonging to the nucleon clouds favours compact, symmetric configurations.

It is interesting to evaluate the effect of the use of a small search cell on the fluctuations also in the general case, i.e. when the fixed grid condition is relaxed. Intuitively, we expect a small effect on the variance, as long as V_{cell} is not too small: the main reduction of fluctuations comes already from the *centroid effect* (see previous Subsection), which is equivalent to an infinitely small step. In fact, the differences between calculations with $V_{cell} = V_p/2$ and $V_{cell} = V_p/4$ (Fig. 5, dotted and dash-dotted curves respectively) are smaller than in the previous calculation with fixed grid. The reduction with respect to the case with $V_{cell} = V_p$ (denoted as “centroid effect” in the Figure) is also smaller.

5.5 Conclusions on the search procedure

In conclusion, it appears from our calculations that the smearing of the nucleon wave packet is rather dependent on the procedure adopted to build nucleons

and is particularly affected by the so-called *centroid effect*, related to the use of randomly distributed test particles for the phase-space mapping. As a consequence, fluctuations calculated in volumes V_p appear reduced. As shown above, the use of a fixed grid to locate the initial and final cells of the colliding test particles would help to increase the value of the variance in V_p . However, energy and momentum conservation would not be exact, due to the phase-space discretization. On the other hand, the standard test particle method allows a good mapping of the phase space and a good resolution of the average collision integral, with perfect energy and momentum conservation. However, when constructing fluctuations, the *centroid effect* may destroy the correlations already built and increase the nucleon cloud smearing. However, the expected statistical value of the fluctuation variance is recovered in large volumes.

This last point has been checked for all the simplified situations considered here (Fermi surface). For instance, this analysis is shown in Fig.6 in the case of the fixed grid with $V_{cell} = V_p$ and test particles randomly distributed inside the system (last case of Section 5.2). Here fluctuations are evaluated in volumes

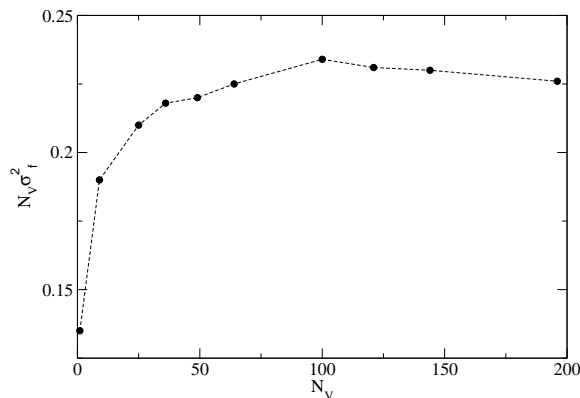


Fig. 6. Variance of the distribution function (rescaled by N_V) as a function of the number N_V of nucleon cells V_p , obtained in the fixed grid case with $V_{cell} = V_p$ and test particles randomly distributed.

V , by considering an ensemble of 800 events. As expected, the fluctuation variance, rescaled by N_V , almost approaches the expected value as the volume V increases. As explained above for the idealized case presented in Fig.3, the maximum value, $N_V \sigma_0^2 = 0.25$, is not exactly reached because of the upper bound imposed to the correlation radius in the nucleon reconstruction procedure and of mass conservation constraints.

6 Non-equilibrium situations

In the Fermi energy domain, two colliding nuclei may be schematically represented by touching Fermi spheres in \mathbf{p} space, so it is interesting to study the development of fluctuations starting from this initial distribution.

In our simplified 2D scheme, we can mimic the two spheres using a “chess-board” initialization, that is subdividing our momentum space in four regions where f is alternatively zero or one. Although the system is in a non-equilibrium situation, the variance, defined as in Eq.(15), starts from its maximum value (since $\langle f \rangle = 0.5$). It can be shown that in the fixed grid case the equilibrium configuration consists of a random distribution of full and empty cells, and the variance keeps constant in time. However, a very different result comes out either changing the search step or removing the fixed grid constraint. In both simulations the variance rapidly decreases because the initial correlation is destroyed by the *centroid effect*.

As an illustrative example, in Fig. 7 we plot σ_f^2 for the choice $V_{cell} = V_p/2$, fixed grid. Comparison with the corresponding curve for the configuration $f(\mathbf{p}) = 0.5 \pm \sigma_f(t = 0)$ (dashed, see Section 5.4) shows that the two calculations converge to the same value. We get a confirmation of these findings

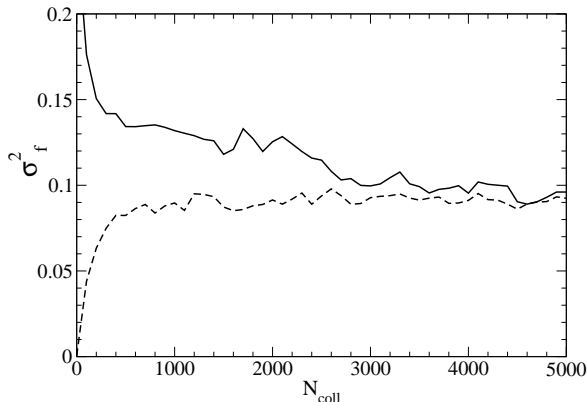


Fig. 7. Comparison between variances obtained with the “chess-board” initialization (solid line) and with the case $f = 0.5 \pm \sigma_f(t = 0)$ (dashed curve) in the fixed grid case for $V_{cell} = V_p/2$.

by removing the fixed grid constraint. Also in this case, at the end we find no difference with the case described before (initialization with randomly distributed test particles, Section 5.3), see Fig. 8. Moreover, in this case the convergence between the two calculations is rather quick. Then we can conclude that the final outcome does not depend on the initial conditions of the system, but only on the final equilibrium situation, as it should be.

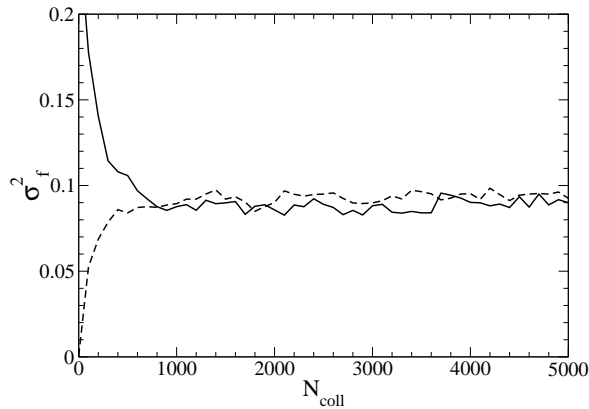


Fig. 8. Comparison between variances obtained with the same initializations of Fig. 7 but for $V_{cell} = V_p$ and without the fixed grid constraint.

7 Results for full 3D simulations

Guided by the simplified schematic cases illustrated above, let us now discuss the full case of a nuclear Fermi gas of particles at a given temperature and density interacting through hard two-body scattering.

As in the previous examples, since we focus on fluctuations in momentum space, only one large cubic cell is present in coordinate space, and all particles can be chosen to collide (no restrictions in \mathbf{r} space). The size of the box is $L = 26 \text{ fm}$, and we consider 2820 nucleons, so that the density has the saturation value $\rho_0 = 0.16 \text{ fm}^{-3}$; each nucleon is represented by a collection of 500 test particles. Besides, we do not consider any distinction between neutrons and protons, so that one nucleon occupies at least a phase-space volume $h^3/4$ ($g = 4$). We initialize the momenta so as to reproduce a Fermi-Dirac profile corresponding to a temperature of 5 MeV . Finally, we consider a constant cross section $\sigma = 160 \text{ mb}$. In these calculations the volume V_{cell} corresponds to a cube of side $l_s = 30 \text{ MeV}/c$ (and coincides with $V_p = h^3/(4L^3)$). We notice that, for the full Fermi gas case, a grid in Cartesian coordinates is easier to use, with respect to spherical coordinates, in the nucleon construction procedure. However, spherical coordinates will be adopted to analyze the resulting fluctuations. Calculations are stopped when the fluctuation variance saturates.

First of all, we checked the effect of our fluctuating collision integral on the average evolution of the system. In Fig. 9 we plot the energy profile of the distribution function at the initial time (solid) and at the time when the fluctuation variance saturates and we stop the calculation (dashed line). Slight changes are observed, probably due to the finite extension of the nucleon packet, that induces a discretization of the phase space.

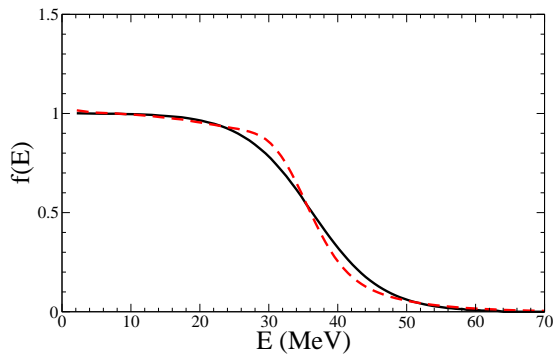


Fig. 9. Distribution function profile at the initial time $t = 0$ (solid) and at the time $t = 100 \text{ fm}/c$ (dashed line).

We also compared the average collision rate with analytical expectations: we find that the number of collisions is slightly larger than the analytical one, but differences are within 10%; on the other hand, similar deviations are also found in usual BUU implementations, due to the approximate mapping of phase space induced by the finite number of test particles.

In the following we analyze in more detail the capability of the procedure to build the fluctuations in the considered 3D scenario. We investigated the region in \mathbf{p} space where collisions are most probable and the extension of the nucleon cloud. From the left panel of Fig. 10 it is evident that most collisions involve nucleons lying on the surface of the Fermi sphere, as expected. Besides, the right panel illustrates the extension of the clouds in the radial direction, calculated according to the definition:

$$\Delta p = \sqrt{\langle (p_i - \langle p \rangle)^2 \rangle_{cloud}}, \quad (16)$$

where $\langle p \rangle$ denotes the center of momentum of the cloud and p_i is the modulus of the momentum of the test particles contained in the cloud.

From this distribution one can deduce that the clouds correspond to a relatively narrow stripe, $2\Delta p \approx 35 \text{ MeV}/c$, in the region where f is different from either zero or one. Moreover, we have checked that the extension of the constructed wave packet is similar in the three directions p_x, p_y, p_z , as expected. We notice also that the tail of the distribution (Fig.10, right) extends up to large Δp values, $\approx 50 \text{ MeV}/c$. Although the nucleon clouds extends, on average, over a volume $(2\Delta p)^3 \sim (35 \text{ MeV}/c)^3$, that is not much larger than V_p , the *centroid effect*, i.e. the fact that the nucleon centroid may be located anywhere, causes a significant smearing of fluctuations, as already discussed in Section 5. In fact, we find that, for our Fermi gas calculations, fluctuations in V_p are considerably underestimated, as shown in Fig.11, where the variance σ_f^2 is reported as a function of the energy $E = p^2/(2m)$. In the following, to test our procedure, we will evaluate fluctuations considering big volumes,

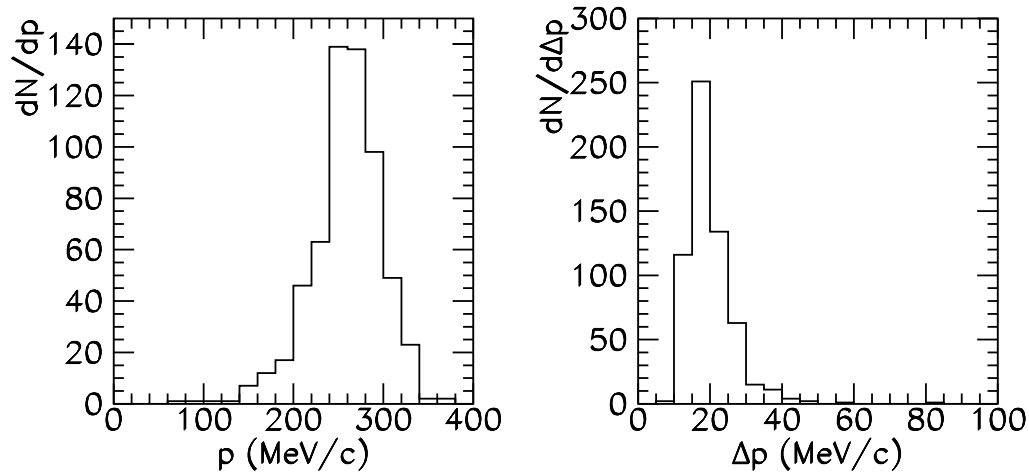


Fig. 10. Left panel: distribution of the position of the centroid of the nucleon “clouds” in the $|p|$ direction. Right panel: distribution of the size of the nucleons on the same axis.

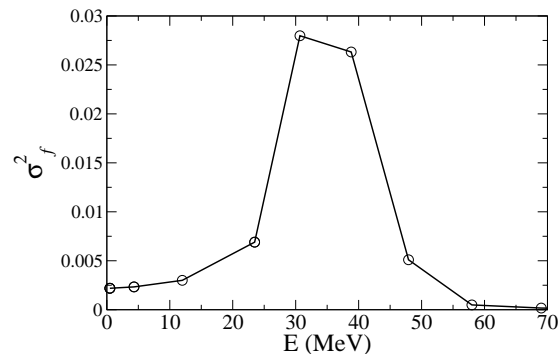


Fig. 11. Profile of the fluctuation variance, as a function of the energy $E = p^2/(2m)$, in cubic cells of size V_p , for a Fermi gas at equilibrium.

that contain many nucleons. However, it should be noticed that, in the geometry considered, it is not trivial to predict which is the size and shape of the most appropriate volume to recover the expected value of fluctuations. While, from one side, it is desirable to consider volumes containing a large number of nucleons, from the other side one should keep in mind that spurious fluctuation reduction, due to the conservation of the total number of particles, may be a problem. Hence we have performed a systematic analysis of fluctuations as a function of the coordinates (p, θ) , integrating over the angle ϕ . The corresponding volume employed for the calculation of the variance is given by:

$$V = 2\pi \frac{\Delta p^3}{3} \Delta \cos \theta$$

We consider volumes corresponding to fixed angular spreads θ and/or to a

given step Δp^3 . In Fig. 12 we fix the angular spread, $\theta = 30^\circ$, and we consider four different steps, Δp^3 , corresponding to different volumes, i.e. to a different number of nucleons N_V that can be contained inside. The consid-

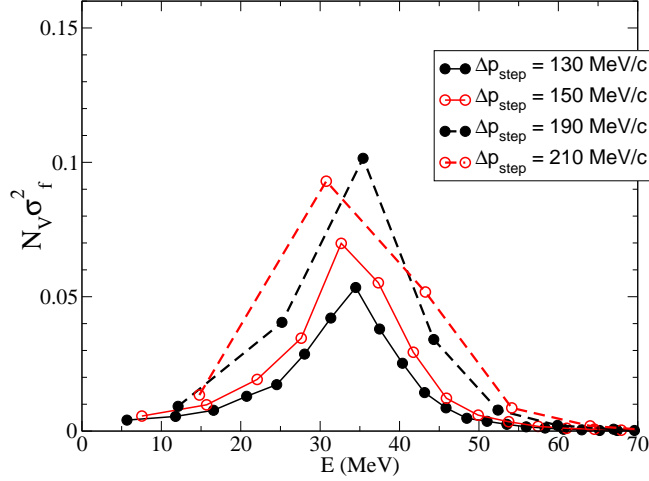


Fig. 12. Fluctuation variance as a function of the energy, for a fixed angular spread $\theta = 30^\circ$ and different steps $\Delta p_{step} = (\Delta p^3)^{1/3}$.

ered volumes can contain up to a rather large number of nucleons (about 90). The variance, multiplied by N_V , is plotted as a function of the energy E . We find that the peak of the variance is around the Fermi energy, as expected. The rescaled variance gets larger when we increase the step Δp^3 . However, even in the best situation, the expected equilibrium value at the peak ($N_V \sigma_0^2 = 0.25$) is underestimated by a factor ~ 2.3 . Therefore, for a fixed value of $\Delta p_{step} = (\Delta p^3)^{1/3} = 190 \text{ MeV}/c$, we tested different angular spreads. In Fig.13 we present the obtained results, rescaled by N_V . Now we can observe

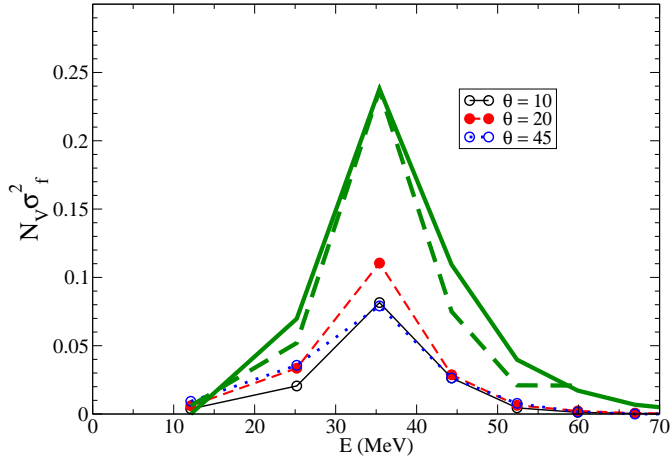


Fig. 13. Fluctuation variance as a function of the energy, for a fixed $\Delta p_{step} = 190 \text{ MeV}/c$ and different angular spreads (curves with circles). The thick full and dashed lines are explained in the text.

that, increasing the angular spread, the variance first increases, then decreases

again, due to the mass conservation constraints. The variance gets larger when considering the angular spread $\theta = 20^\circ$, but the expected value is still underestimated by about a factor 2, at the peak. This result can be understood on the basis of the results obtained in V_p and displayed in Fig.11. In fact, in order to recover the expected fluctuation value, the volume employed for the calculation of the variance must be much larger than $V_p^{1/3}$ in all the directions $(p, \cos(\theta), \phi)$. Due to the considered geometry, while this can be achieved in the angular coordinates, this cannot be easily obtained along the p direction without losing locality for the value of f and related fluctuations. Actually, in the case of $\Delta p_{step} = 190 \text{ MeV}/c$, the corresponding extension along the p direction, Δp_{mod} , of the volume considered to evaluate the function f is approximately equal to $30 \text{ MeV}/c = V_p^{1/3}$ at $p = p_F$. We thus expect fluctuations to be reduced, with respect to $f_{eq}\bar{f}_{eq}$, by a factor $\alpha^{1/3} \approx 0.48$, being $\alpha \approx 0.11$ the reduction factor in V_p , as evaluated from Fig.11. The expected fluctuation reduction can be extracted also from the schematic calculations described in Sect.5. In fact, from the inspection of Fig.4, it appears that, in the fixed grid scheme, fluctuations in V_p are reduced by a factor 0.56. Relaxing the fixed grid constraint in one dimension, fluctuations are further reduced by a factor 0.64 with respect to the fixed grid case. We thus expect a fluctuation reduction by a factor $0.56^{1/3} \times 0.64 \approx 0.5$ (at the Fermi surface). This is close to our result at $E = E_F = p_F^2/(2m)$ (see the dashed line with circles in Fig.13, for instance).

One may try to introduce this correction in the results of Fig. 13. In the considered geometry, the reduction factor α of the fluctuations in V_p depends on the energy E , i.e. one can write, for the variance in V_p :

$$\sigma_f^2(E, N_V = 1) = F(E) \alpha(E), \quad (17)$$

where $F(E)$ indicates the expected fluctuation value, that in our case should coincide with $f_{eq}\bar{f}_{eq}$.

By approximating the volume dependence of the rescaled variance by a linear behaviour for small volumes (see Fig.3 for instance), the fluctuation variance presented in Figs. 12-13 can be rewritten as:

$$N_V \sigma_f^2(E, N_V) \approx F(E) \alpha^{1/3}(E) \frac{\Delta p_{mod}}{V_p^{1/3}}. \quad (18)$$

We notice that Δp_{mod} is also depending on E .

Eqs.(17)(18) allow to extract the suppression factor $\alpha(E)$, as well as the function $F(E)$. The latter is displayed in Fig.13 (thick dashed line). One can see that the expected fluctuation value, $f_{eq}\bar{f}_{eq}$ (thick solid line), is well reproduced at the Fermi surface, while it is underestimated, within 30%, especially for outer regions. This underestimation indicates that in our procedure, due

to the finite extension of the nucleon cloud, the regions far from the Fermi surface are less involved in the building of fluctuations than they should be and can be considered as an intrinsic limitation of the method.

However, the overall shape of the fluctuation variance is reasonably reproduced, relative to $f\bar{f}$: This is a nice indication that the Pauli blocking is effective, and the equilibrium distribution is almost unchanged by the procedure. Therefore, it really represents a remarkable improvement with respect to the original method by Bauer et al. (see Ref.[29]), which makes us confident about applications to nuclear reactions.

We can directly visualize the effect of the fluctuating term by selecting a thin region in momentum space around the Fermi momentum. For this purpose, we adopt a new set of coordinates $(dp, p d\theta, p \sin(\theta) d\phi)$; for fixed p and dp , the distribution function depends only on two coordinates, namely:

$$f(p, \theta, \phi) \rightarrow f(\theta, \eta)$$

with $\eta = \sin(\theta)\phi$. This set of coordinates correspond to displacements of equal length along the three directions: p, θ, ϕ . We choose $p = 260 \text{ MeV}/c$ (approximately equal to the Fermi momentum) and $dp = 10 \text{ MeV}/c$, and in Fig. 14 we plot the distribution function $f(\theta, \eta)$ at two different times (initial and final times). We recognize the sinusoidal profile on the η axis due to the modulation given by the $\sin(\theta)$ factor. At the initial time, f is nearly uniform, and its fluctuations are simply due to the numerical noise induced by the finite number of test particles. At later times, we observe the growth of fluctuations, evidenced by the typical structure with “peaks and holes”.

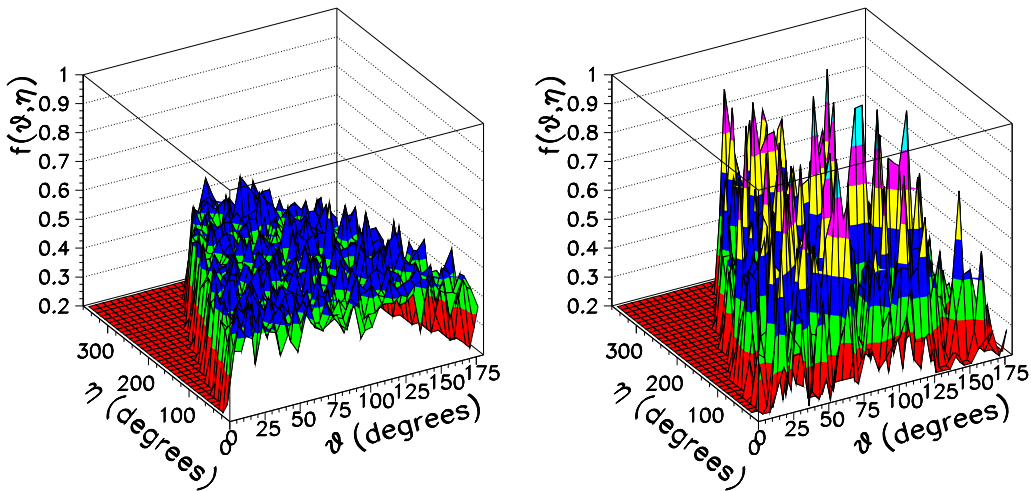


Fig. 14. Distribution function $f(\theta, \eta)$ at time $t = 0$ (left) and $t = 100 \text{ fm}/c$ (right).

8 Methods to increase fluctuations in V_p

In actual nuclear collisions the extension of the nucleon wave packet in phase-space may affect the transport dynamics and it may be important to correlate the test particles belonging to the nucleon clouds inside smaller volumes. In the context of the simplified model (Fermi surface) discussed in Sect.5 we attempted to find a method to reduce the nucleon cloud smearing and enhance the fluctuations in V_p without losing the consistency of the original procedure.

First of all, it should be remembered that the collision probability is given by $f(\mathbf{p}_1)\bar{f}(\mathbf{p}_3)$ (see Sect. 5.1): therefore, we need to consider only two locations in \mathbf{p} space. The main idea is to force the system to fully empty the cells associated with the initial state or fully fill the final state when a collision occurs. This condition is not automatically achieved for all cells contributing to a given collision. In fact, the number of particles, $n_t(i)$, taken from a cell i and employed to build the nucleon obey to the constraint:

$$\sum_i n_t(i) = N_{test}$$

being N_{test} the number of test particles per nucleon. Hence the number of test particles that are really taken from a cell is not always equal to $n_t = \min(n_1, \bar{n}_3)$, but instead to $n'_t = \min(n_t, n_{res})$, being

$$n_{res}(i) = N_{test} - \sum_{i'=1}^{i-1} n_t(i') \quad (19)$$

The idea is to try to avoid the situation when the number of particles moved is less than n_t . In this way fluctuations get to a larger value, since we favour the transitions where cells are completely filled or emptied. In order to implement this idea, when constructing the nucleon clouds we choose, among the possible ones, the cells for which the probability $p_t = \frac{n'_t}{n_t}$ is large.

The outcome of this method is plotted in Fig. 15 for the fixed grid case, where the result of Fig. 4 is also shown for comparison (solid line). As the dashed curve in Fig. 15 clearly shows, this optimization procedure is successful in enhancing the fluctuations, which eventually reach almost their upper limit $\sigma_0^2 = 0.25$. Actually, this maximum value is not obtained due to the fact that only adjacent cells are considered in the nucleon construction. In this way, some half-filled cells remain “isolated” and are not involved in a collision anymore. Indeed, at the time when we stop the calculation, isolated cells amount to about 5% of the total.

The method works also in more general situations, for instance in the case corresponding to fluctuating initial conditions (see Sect.5.2). The comparison between variances with and without the optimization procedure is shown in

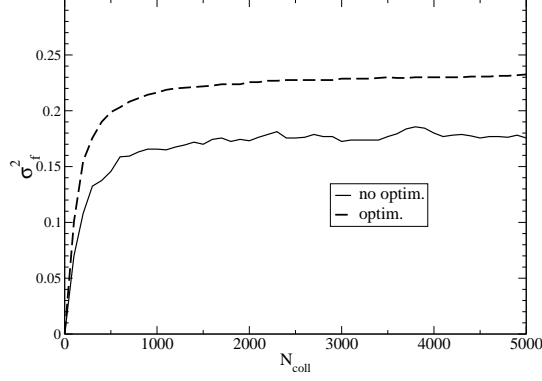


Fig. 15. Variance of the distribution function in V_p , as a function of the number of collisions, in the fixed grid scheme. Solid line: no optimization; dashed line: optimized procedure.

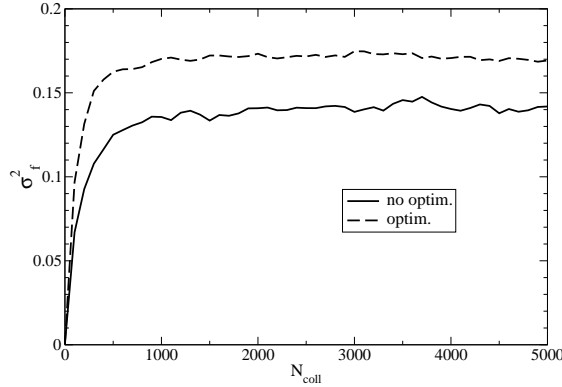


Fig. 16. Variance of the distribution function in V_p , as a function of the number of collisions, in the fixed grid scheme with fluctuating initial conditions. Solid line: no optimization; dashed line: optimized procedure.

Fig. 16. As in the previous case, the optimization favours a faster growth of the fluctuations. Their saturation value for $V = V_p$ is now enhanced, by $\sim 20\%$ with respect to the standard procedure. This is an indication that the procedure is able to increase the number of empty and full cells. This feature is also evident from the distribution of values of f plotted, for the same two simulations of Fig.16, in Fig. 17.

In the end, this procedure helps the nucleon packets to keep a similar, more compact shape in \mathbf{p} space during the time evolution of the system, from one collisional event to another. As a consequence, nucleons are more localized and fluctuations in V_p appear enhanced.

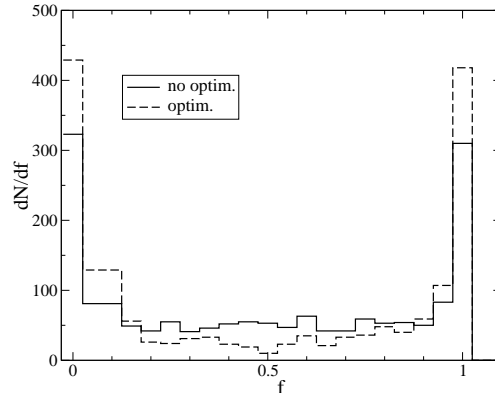


Fig. 17. Distribution of the number of cells as a function of their occupation f for the same two calculations of Fig. 16.

9 Conclusions

We have proposed a new numerical implementation of the full Boltzmann-Langevin equation in 3D. The stochastic character of the two-body collision integral, that in standard transport codes applies only to the single test particles, leading to a strong reduction of fluctuations, is recovered, at the nucleon level, by a careful reconstruction of the nucleon wave packet once collisions occur. This is achieved by moving, in each collisional event, two entire test particle clouds, corresponding to one nucleon each, as proposed in Ref.[23]. However, while in the original procedure the Pauli blocking was checked only for the centroids of the nucleon clouds, here we propose a new method that allows to construct nucleon wave packets by carefully checking the Pauli blocking for the entire swarm of test particles. The last point is essential in the construction of the correct fluctuation value in fermionic systems. The nucleon wave packet may take, in principle, any shape. Thus the correlation volume, i.e. the volume of the sphere that contains all test particles that move together is generally larger than h^3 . Moreover, the nucleon centroid is chosen randomly among the test particle distribution, leading to a partial overlap of nucleon configurations from one collision to another. All these effects lead to a reduction of fluctuations in the cells of volume h^3 . However, the correct fluctuation value is recovered in larger volumes, where all possible nucleon configurations may be accommodated.

The procedure, and its numerical ingredients, has been tested carefully in several idealized situations, studying in particular the relation between the results obtained for the fluctuations in cells of volume h^3 and the ingredients of the model. Considering a fermionic system at equilibrium, at a given density and temperature, we find that our procedure builds, within a good approximation, the expected profile of the fluctuation variance, $f_{eq}\bar{f}_{eq}$, as a function of the nucleon energy. This can be considered as a significant improvement with

respect to the original procedure [23], that opens interesting possibilities of applications to nuclear collisions. In fact, the method proposed can be easily implemented into existing transport codes, and could allow to treat, in a more complete way, phenomena where large fluctuations or bifurcations occur and fluctuations are important.

Finally we stress that the results presented here are relevant not only for nuclear fragmentation studies, but in general for the dynamical description of quantum many-body systems.

Acknowledgments We warmly thank H.H.Wolter for the reading of the manuscript and stimulating discussions.

References

- [1] G.F.Bertsch and S.Das Gupta, Phys. Rep. **160** (1988) 189
- [2] A.Bonasera, F.Gulminelli and J.Molitoris, Phys. Rep. **243** (1994) 1
- [3] R.Botet et al., Phys. Rev. Lett. **86** (2001) 3514
- [4] J.B.Elliott et al., Phys. Rev. Lett. **88** (2002) 042701
- [5] M.D'Agostino et al., Nucl. Phys. **A699** (2002) 795.
- [6] Ph.Chomaz and F.Gulminelli, Nucl. Phys. **A647** (1999) 153; F.Gulminelli, Ph.Chomaz, Al.H.Raduta, Ad.R.Raduta, Phys.Rev.Lett. **91** (2003) 202701
- [7] G.Tabacaru et al., Eur. Phys.J. **A18** (2003) 103
- [8] Ph.Chomaz, M.Colonna, J.Randrup, Phys. Rep. **389** (2004) 263
- [9] A.Ono, Phys. Rev. **C59** (1999) 853
- [10] J.Aichelin, Phys. Rep. **202** (1991) 233
- [11] H.Feldmeier, Nucl.Phys. **A515** (1990) 147
- [12] A.Ono, H.Horiuchi, T.Maruyama and A.Ohnishi, Phys. Rev. Lett. **68** (1992) 2898; A.Ono, H.Horiuchi, T.Maruyama and A.Ohnishi, Prog. Theor. Phys. **87** (1992) 1185.
- [13] M.Papa, T.Maruyama, A.Bonasera, Phys. Rev. **C64** (2001) 024612
- [14] M.Colonna and Ph.Chomaz, Phys. Lett. **B436** (1998) 1
- [15] J.Rizzo, M.Colonna, A.Ono, Phys. Rev.**C76** (2007) 024611

- [16] S.Ayik, C.Gregoire, Phys. Lett. **B212** (1998) 269, and refs. therein.
- [17] J.Randrup and B.Remaud, Nucl. Phys. **A514** (1990) 339
- [18] Ph.Chomaz, G.F.Burgio, and J.Randrup, Phys.Lett. **B254** (1991) 340
- [19] G.F.Burgio, Ph.Chomaz, and J.Randrup, Nucl. Phys. **A529** (1991) 157
- [20] E.Suraud et al., Nucl. Phys. **A542** (1992) 141; E.Suraud et al., Nucl. Phys. **580** (1994) 323; F.S.Zhang and E.Suraud, Phys. Rev. **C51** (1995) 3201
- [21] M.Colonna et al., Nucl. Phys. **A642** (1998) 449
- [22] P.Chomaz, M.Colonna, A.Guarnera, et al., Phys. Rev. Lett. **73** (1994) 3512;
A.Guarnera, Ph.Chomaz, M.Colonna, J.Randrup, Phys. Lett. **B403** (1997) 191
- [23] W.Bauer, G.F.Bertsch, and S.Das Gupta, Phys. Rev. Lett. **58** (1987) 58
- [24] L.W. Nordheim, Proc. R. Soc. London **A119** (1928) 689
- [25] E.A. Uehling and G.E. Uhlenbeck, Phys.Rev. **43** (1933) 552
- [26] W. Bauer, G.F. Bertsch and H. Schultz, Phys.Rev.Lett. **69** (1992) 1888
- [27] B. Borderie, B. Remaud, M.F. Rivet and F. Seville, Phys.Lett. **B302** (1993) 15
- [28] B. A. Li and W. Bauer, Phys. Lett. **B254** (1991) 335; Phys. Rev. **C44** (1991) 450
- [29] F. Chapelle, G.F. Burgio, Ph. Chomaz, and J. Randrup, Nucl. Phys. **A540** (1992) 227
- [30] G.F. Burgio, Ph. Chomaz, and J. Randrup, Phys. Rev. Lett. **69** (1992) 88
- [31] P.G. Reinhard and E. Suraud, Ann. of Phys. **216** (1992) 98; P.G. Reinhard and E. Suraud, Nucl. Phys. **A545** (1992) 59c